Earthquake Geotechnical Engineering for Protection and Development of Environment and Constructions – Silvestri & Moraci (Eds)
© 2019 Associazione Geotecnica Italiana, Rome, Italy, ISBN 978-0-367-14328-2

Kinematic interaction of pile groups with liquefied soil during lateral spreading based on 1g shake table tests

A. Kavand & M. Yazdi
School of Civil Engineering, College of Engineering, University of Tehran, Tehran, Iran

ABSTRACT: In this study, a number of 1g shake table tests are conducted to investigate the variation of bending moments in individual piles of the pile groups with different configurations subjected to liquefaction-induced lateral spreading. Time histories of accelerations and excess pore water pressures in the free field part of the soil, displacements of piles as well as bending moments in piles were recorded during the experiments which are presented and discussed in this paper. The results demonstrate that the amount of developed bending moments in piles configured in a group differs from those observed for a single pile. Moreover, the bending moments vary in individual piles of the group depending on their position within the group. In conclusion, considering these differences can lead to a more efficient and economical design of the piles, particularly when the pile group consists of a large number of piles.

1 INTRODUCTION

There are numerous cases in which important structures supported on pile foundations have been severely damaged due to liquefaction during the past earthquakes. These damages have been more severe in gently sloping grounds where liquefaction has led to large lateral displacements of the ground or liquefaction induced lateral spreading. These large lateral ground displacements can exert considerable lateral forces on deep foundations. In this regard, there are a number of well-known examples of severely damaged piles due to lateral spreading such as the ones observed during the 1964 Niigata, Japan, the 1989 Loma Prieta, USA, the 1995 Kobe, Japan, the 2010 Haiti and the 2011 Tohoku Pacific, Japan, earthquakes. Based on these observations, damages to the piles have been concentrated in three specific locations including the connection of the piles to the cap, the boundary between the liquefiable and the base non-liquefiable layers and the boundary between the liquefiable and the upper non-liquefiable layers (Abdoun & Dobry 2002, Cubrinovski et al. 2017, Tokimatsu 1999).

To better understand the mechanism of soil-pile-interaction during lateral spreading, researchers have utilized different methods including numerical modeling, centrifuge tests (e.g. Brandenberg et al. 2005), 1g shake table tests (e.g. Haeri et al. 2012, Kavand et al. 2014) and field investigations (e.g. Jayasinghe et al. 2018, Juirnarongrit & Ashford 2006). In this respect, physical modeling can play an effective role in investigating the mechanisms of soil-pile interaction in laterally spreading ground. In this study, a set of 1g shake table tests were conducted to investigate the extent of lateral loads exerted on pile groups with different configurations due to liquefaction induced lateral spreading.

2 SHAKE TABLE TESTS

This study was performed using the 1g shake table at the Physical Modelling Laboratory of the School of Civil Engineering, University of Tehran. The shake table is 1.8m long and 1.2m wide, and it is capable to impart base motions with a maximum acceleration of 1g (for a payload of 5 tons) and within a frequency range between 0.01Hz and 25Hz. A rigid box made of

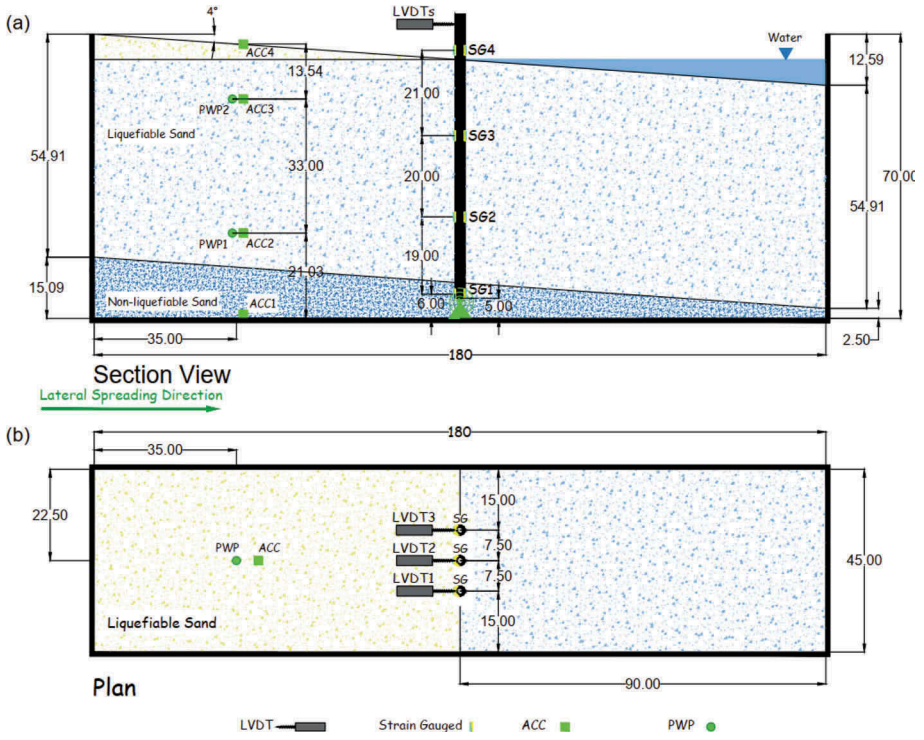

Figure 1. Plan and cross sectional views of a physical model test on a group of piles (without a cap) arranged perpendicular to the direction of lateral spreading

Plexiglas was used as the physical model container. The box was 1.8m long, 0.45m wide and 0.7m high. Figure 1 shows the schematic plan and cross sectional views of one of the experiments of the study.

As it can be seen in Figure 1, the model ground consists of two sandy layers with a slope of 4 degrees. The sand used for the construction of these layers is Firoozkuh silica sand No. 161 whose geotechnical properties are summarized in Table 1. The top liquefiable layer is 0.55m thick with a relative density of 10% overlying a non-liquefiable layer with a relative density of 70%. Both of the aforementioned layers are constructed by controlled tamping of the moist sand. The configurations of piles in all the experiments are depicted in Figure 2. All piles were designed based on JRA code in prototype scale and subsequently were scaled down to model scale using the similitude laws proposed by Iai et al. (1989). A geometric scale of l=15 was used for this purpose. In Table 2, the geometrical and mechanical properties of the model piles are presented. It should be noted that all physical models were subjected to a sinusoidal base excitation with an amplitude of 0.3g and frequency of 6Hz. The duration of the base motion was 12.0 sec. Two photographs showing one of the physical models of the current study on the shake table are shown in Figure 3.

Table 1. Geotechnical properties of Firoozkuh silica sand no.161

Specific gravity	Maximum void ratio (e_{max})	Minimum void ratio (e_{min})	Coefficient of uniformity (C_u)	Mean grain size (D_{50}) (mm)	D_{10} (mm)	D_{90} (mm)
2.65	0.870	0.608	1.49	0.24	0.18	0.39

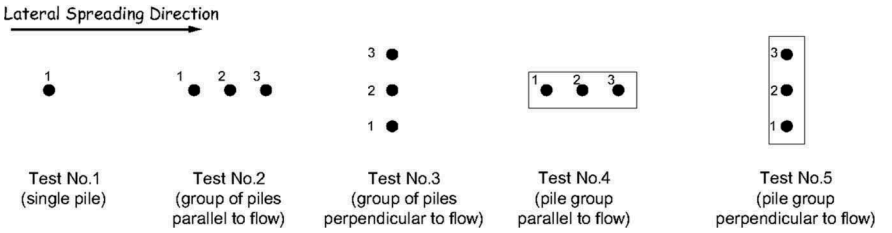

Figure 2. Schematic representation of configuration of piles in all experiments of the current study

Table 2. Geometrical and mechanical properties of the model piles

Material	Height (cm)	Outer diameter (mm)	Thickness (mm)	I (mm^4)	EI($N.m^2$)
Aluminum	70	25	0.7	3947.63	283.61

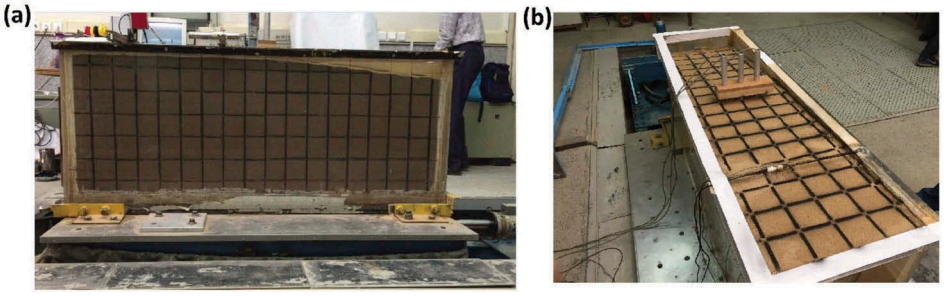

Figure 3. One of the physical models of the current study on the shake table: (a) front view (b) top view

3 GENERAL EXPERIMENTAL RESULTS

In this section, a summary of the experimental results including time histories of accelerations, excess pore water pressures, pile cap displacements and bending moment in piles are presented. The results of Test no.3 are presented as an example. At the end, the bending moments in piles in different tests are compared and the results are discussed.

3.1 *Soil acceleration records in free field*

Typical time-histories of soil acceleration in the free field part of the model are demonstrated in Figure 4 for Test no. 3. As it can be seen, the amplitude of recorded accelerations in the liquefiable layer decreases significantly at the early stages of shaking due to the loss of shear strength of the soil. The acceleration spikes observed after liquefaction are attributed to the dilative behavior of the soil.

3.2 *Excess pore water pressure records in free field*

Variations of pore water pressure were monitored during the test by installing PWP transducers at different depths of the free field part of the model. In Figure 5, typical time histories of pore water pressures are presented for Test no. 3. As it is clear, after a few cycles of shaking, the pore water pressure increased remarkably and became equal to the corresponding initial effective vertical stress indicating liquefaction in soil. Moreover, liquefaction occurred sooner at shallower depths while the dissipation of the excess pore water pressures started from the bottom towards the top of the liquefiable soil.

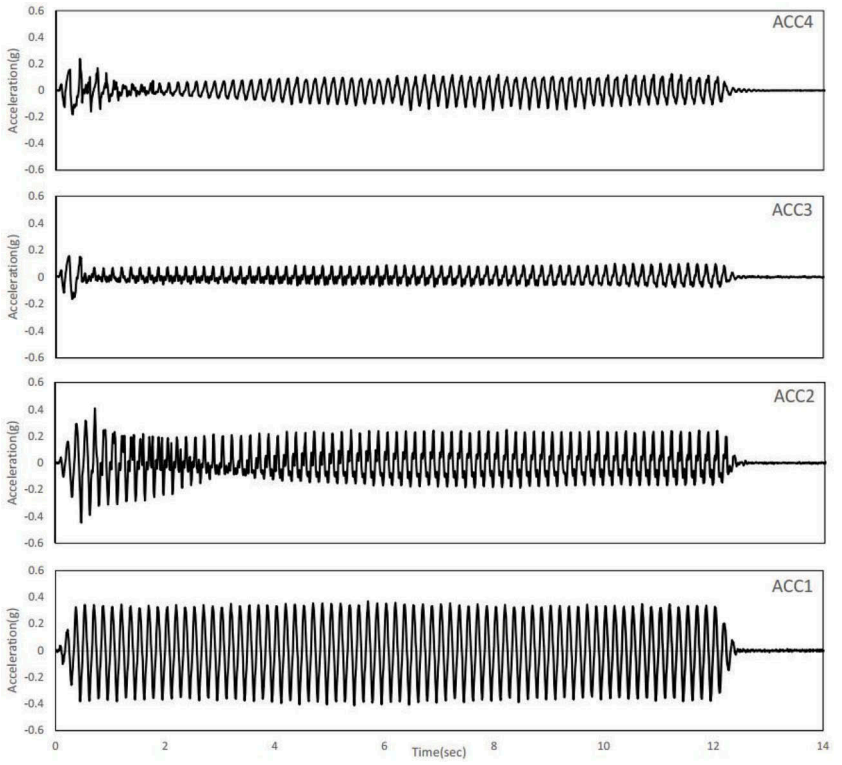

Figure 4. Typical time histories of acceleration of soil in free field for Test no.3

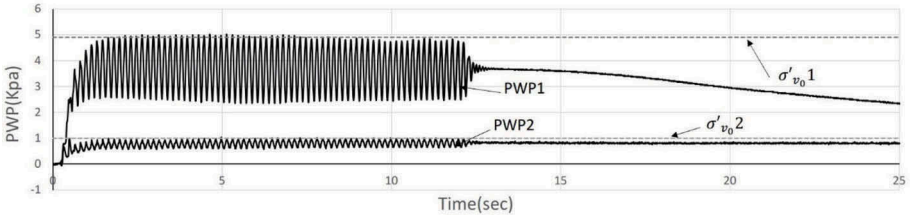

Figure 5. Typical time histories of excess pore water pressure in free field for Test no.3

3.3 *Pile head displacement records*

Figure 6 shows the lateral displacement record of the head of pile 1 in Test no. 3 as an example. In this figure, the positive values represent the movement of the pile downslope. According to this figure, upon the lateral movement of liquefied soil downslope, substantial lateral forces were exerted on the pile. Therefore, the pile displacement reached a peak value. Then, the elastic force in pile overcame the shear strength of the liquefied soil, so the pile returned towards the upslope and the pile displacement decreased.

3.4 *Bending moment in piles*

Time histories of bending moments are obtained by installing stain gauges at different elevations of the piles. The depths at which strain gauges are installed are presented in Figure 1. To eliminate the axial strains, a Wheatstone half-bridge was used and configured to cancel out

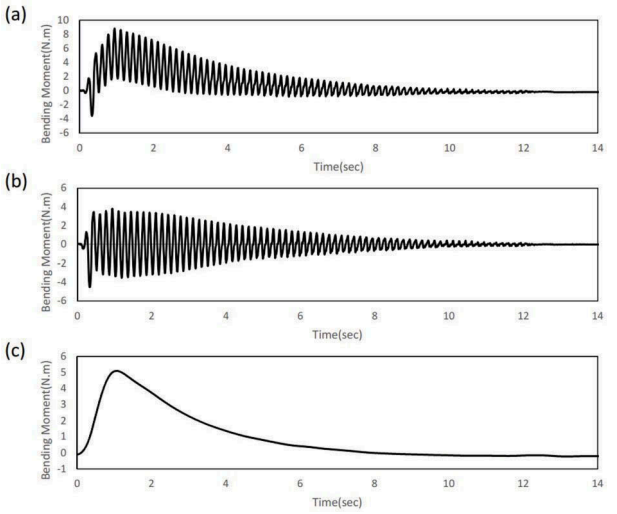

Figure 6. A sample time history of pile head displacement (pile1 in Test no. 3)

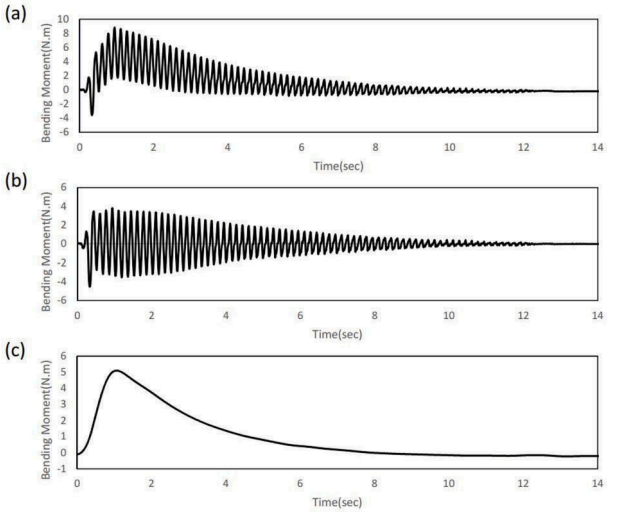

Figure 7. Time history of bending moment in pile 1 of Test no.3 at the base of liquefiable layer: (a) originally recorded (b) cyclic component (c) monotonic component.

the axial strains while maintaining the strains due to bending moments. The bending moments were calculated using Equation 1.

$$M = \frac{E.V.C_c.I}{C} \tag{1}$$

where V is the output voltage, C_c is the calibration coefficient, E is the modulus of elasticity, I is the moment of inertia of the pile, C is the distance between the neutral axis of the pile section and the outer surface of it and M is the bending moment in pile.

Since the aim of this paper is to investigate the bending moments induced by lateral spreading, the monotonic component of bending moments should be determined. For this purpose,

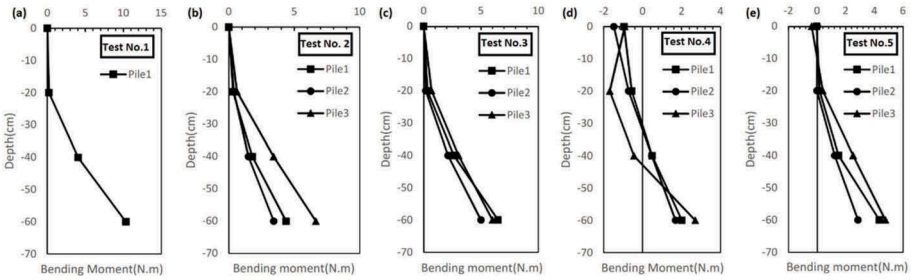

Figure 8. Profiles of the maximum bending moments in the model piles

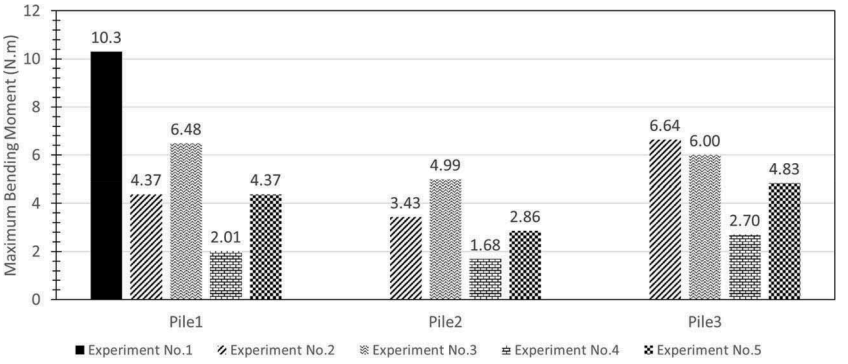

Figure 9. Maximum values of bending moments at the base of the model piles

the monotonic bending moments were extracted from the recorded bending moments using Equation 2. The outcome of this procedure is shown in Figure 7 for pile 1 in Test no.3.

$$M(z,t)_{monotonic} = M(z,t) - M(z,t)_{cyclic} \tag{2}$$

Figure 8 demonstrates the profiles of bending moments in piles when the bending moments at the base of the pile reach their maximum values. As seen, the single pile behaves like a cantilever beam showing an increasing trend of bending moment with depth. The variation of bending moments with depth in piles of Tests no.2 and no.3 also show a cantilever behavior. However, in Tests no. 4 and no.5, the bending moment near the pile cap is negative while its value near the base of the pile is positive. This behavior results from the effects of the fixity imposed by the pile cap at the top of the piles.

The maximum values of bending moments in all model piles are compared in Figure 9. According to this figure, the single pile experienced the largest bending moment and when the piles are configured in groups, the amount of bending moment in them decreases as they interact with each other. In Test no.2 in which the piles were arranged parallel to the lateral spreading direction, the middle pile receives less forces than the two upslope and downslope ones due to the shadow effect and the downslope pile shows the greatest bending moment values as the liquefied soil behind it moves laterally, therefore the pile loses its lateral support. In Test no.3 where the group of piles were configured perpendicular to the direction of lateral spreading, less lateral pressure is exerted on the middle pile due to neighboring effect. This observation was also reported by Haeri et al. (2012). When the pile cap is added to the model, the variation of maximum bending moments in different piles of the group is similar to what observed for pile groups without a cap (i.e. Tests no. 2 and no.3). In addition, when the piles

are configured perpendicular to the lateral spreading direction, they experience larger bending moments comparing to the case that they are arranged parallel to the lateral spreading direction. The reason is that in latter case, the piles receive more lateral forces as the area subjected to lateral movement of the liquefied soil is greater.

4 CONCLUSION

This paper addresses the kinematic interaction of piles having different configurations with the liquefied soil during lateral spreading. The main findings of the current paper are highlighted below:

1. The amplitude of the accelerations decreases considerably after liquefaction due to the loss of shear strength of the soil.
2. After liquefaction, the soil moves downslope and exerts considerable lateral pressure on the piles leading to development of bending moments in them. The bending moments in piles attain a peak value and then decrease as the elastic forces in the piles overcome the shear strength of the liquefied soil which allows the piles to gradually move upslope again.
3. The largest bending moment is observed in the single pile whereas the pile groups (with or without a cap) show smaller bending moments due to the interaction of individual piles in the group. In addition, when the piles are configured perpendicular to the lateral spreading direction, larger bending moments are induced in them comparing to the case that they are installed parallel to the lateral spreading direction.
4. Based on the position of an individual pile in the group, the amount of induced bending moments in them varies. When the piles are configured parallel to the lateral spreading direction, the bending moments in the middle pile are smaller than those induced in both upslope and downslope piles. Moreover, when the piles are configured perpendicular to the lateral spreading direction, the bending moment in the middle pile is lower than that in the side piles due to the neighboring effect. For the pile group (with a pile cap) arranged parallel to the direction of lateral spreading, the magnitude of induced bending moments in the piles increases by moving from upslope to downslope.

REFERENCES

Abdoun T, Dobry R. 2002. Evaluation of pile foundation response to lateral spreading, *Soil Dynamics and Earthquake Engineering* 22, 1051–1058.

Brandenberg S, Boulanger R, Kutter B, Chang D. 2005. Behaviour of pile foundations in laterally spreading ground during centrifuge test, *Journal of Geotechnical and Geoenvironmental Engineering*, 131(11),1378–1391.

Cubrinovski M., Bray J., de la Torre C., Olsen M., Bradley B., Chiaro G., Stock E., Woth-erspoon L. 2017. Liquefaction effects and associated damages observed at the Welling-ton Centre port from the 2016 Kaikoura earthquake. Bulletin of the New Zealand Society for Earthquake Engineering 50(2):152–173.

Haeri S.M., Kavand A., Rahmani I., Torabi H. 2012. Response of a group of piles to liquefaction-induced lateral spreading by large scale shake table testing, *Soil Dynamics and Earthquake Engineering* 38, 25–45.

Iai S., Tobita T. and Nakahara T. 2005. Generalized scaling relations for dynamic centrifuge tests, *Geotechnique* 55(5), 355–362.

Japan Road Association (JRA) 2002. Seismic design specifications for highway bridges. English version, Prepared by Public works Research Institute (PWRI) and Ministry of Land, Infrastructure and Transport, Tokyo, Japan.

Jayasinghe L.B., Zhao Z.Y., Goh A.T.C., Zhou H.Y., Gui Y.L., Tao M. 2018. A field study on pile response to blast-induced ground motion. *Soil Dynamics and Earthquake Engineering* 114, 568–575.

Juirnarongrit T. and Ashford S.A. 2006. Soil-Pile response to blast-induced lateral spreading. II: Analysis and Assessment of the p-y method, *Journal of Geotechnical and Geoenvironmental Engineering*, ASCE 132(2), 163–172.

Kavand A, Haeri SM, Asefzadeh A, Rahmani I, Ghalandarzadeh A, Bakhshi A. 2014. Study of the behavior of pile groups during lateral spreading in medium dense sands by large scale shake table test. *International Journal of Civil Engineering*. 12(3), 374–391.

Tokimatsu K. 1999. Performance of pile foundations in laterally spreading soils, *Proceedings of the Second International Conference on Earthquake Geotechnical Engineering* 3, 64–957.